# Syntheses of Square Planar Gallium Complexes and a Proton NMR Correlation Probing Metalloaromaticity

Thomas M. Bass, Cody R. Carr, Tobias J. Sherbow, James C. Fettinger, and Louise A. Berben\*

Department of Chemistry, University of California, Davis, California 95616, United States

**ABSTRACT:** Syntheses of square planar (SP) coordination complexes of gallium(III) are reported herein. Using the pyridine diimine ligand (PDI), we prepared both (PDI<sup>2</sup>-)GaH (4) and (PDI<sup>2</sup>-)GaCl (5), which were spectroscopically and structurally characterized. Reduction of PDI using Na metal afforded "Na<sub>2</sub>PDI", which reacts with in situ-prepared "GaHCl<sub>2</sub>" or GaCl<sub>3</sub> to afford the SP 4 and 5. The planar geometry of these and previously reported SP Al(III) complexes is attributed to energetic stabilization derived from a ring-current effect, or metalloaromaticity. Typically, aromaticity in metal-containing ring systems can be difficult to characterize or confirm experimentally. An experimental approach employing proton NMR spectroscopy and described here provided an estimate of a downfield chemical shift promoted by a small ring-current associated with metalloaromaticity. Near infra-red spectroscopic analyses display ligand-metal charge transfer bands which support the assignment of aromaticity. The SP complexes (PDI<sup>2</sup>-)AlH (1), (PDI<sup>2</sup>-)AlCl (2), (PDI<sup>2</sup>-)AlI (3), 4, and 5 are all discussed in this report, using aromaticity as a model for their electronic structure and reactivity properties.

The chemistry of Group 13, in particular of aluminum, is undergoing rapid development across multiple applications and across different classes of compound. One area seeing recent interest is in low-valent Al compounds, where the synthesis of nucleophilic aluminyls has uncovered the ability to activate substrates like benzene that are usually unreactive.<sup>2</sup> Frustrated Lewis pair chemistry continues to be developed and that work also includes Al-derived Lewis acids in some instances.3 Ligand-based redox chemistry has seen advances that are enabled by the stability of the +3 oxidation state in Group 13 ions toward reduction: metal-ligand complexes of Al and Ga that support up to six successive ligand-based couples are now known and applied in energystorage technologies, and in delocalized and tunable mixedvalent compounds. 4 The subject of this report is the planar redox-active ligand complexes of Group 13 which have aromatic character and which promote facile ligand-based proton transfer chemistry and NADH+-like hydride chemistry.5

Aromaticity is best-known in benzene and in main group ring systems such as P5-, where the Hückel description, a ring with  $(4n + 2) \pi$ -electrons, is easily understood. The nuanced physical properties of aromatic compounds such as benzene are richer than the definition and explain unusual aspects of those compounds chemical reactivity and spectroscopic signatures. 6,7 These signatures of aromaticity, include the planar structure, the carbon-carbon bond lengths that are similar rather than alternating single and double, and the "ring current" which is most easily observed using proton NMR spectroscopy to uncover and quantify the deshielding of protons. The resonance stabilization results in unusual reactivity characteristics of aromatic compounds such as the electrophilic substitution of benzene. Ring current effects are easily observed in main group aromatic compounds because the NMR chemical shifts caused by deshielding are large. As examples, the cyclic P5- and P2N3anions have <sup>31</sup>P-NMR chemical shifts consistent with a ring

current at 470 and 467.2 ppm, respectively,<sup>8,9</sup> and benzene has <sup>1</sup>H-NMR chemical shift of 7.2 ppm. Even without the direct "non-aromatic" analog of each of these molecules in hand we are convinced of the ring current existence.

In contrast, the ring current in metal-containing aromatic rings can be quite small and aromaticity in metal ligand complexes such as square planar (SP) coordination complexes can easily go unnoticed.7 Opportunities to rationalize, predict, and tune the reactivity, electronic structures, and materials properties of metal-containing aromatic ring complexes, and to employ them in productive applications are missed when aromaticity goes undetected. Enhanced nucleophilicity of ligand atoms as potential reaction sites are one possible manifestation of an aromatic electronic structure,10 as is near infra-red luminophore behavior and large Stokes shifts in emission spectra, as reported for aromatic osmapentallene complexes. 11 Gray and Balhausen experimentally determined ring current effects in SP Ni dithiolene coordination complexes by single crystal magnetic susceptibility measurements. 12,13 However, most discussions of aromatic metal-containing molecules rely on theoretical methods to validate their assignment as aromatic. These instances include Group 13 analogs of the tropylium cation borepin, aluminepin, and gallepin,14 aluminabenzene, 15 the osmacycles, 16 and the plumbole and stannole analogs of cyclopentadienyl. 17

In this work, synthesis of the first SP Ga compounds are reported: (PDI²-)GaH (4), and (PDI²-)GaCl (5). Their properties are described using the aromatic electronic structure model as a framework, along with the properties of previously reported SP (PDI²-)AlH (1) and (PDI²-)AlCl (2),5b,18 and newly prepared (PDI²-)AlI (3). We also describe a simple analysis method based on proton NMR spectroscopy to probe aromatic ring current effects on chemical shift, even when the "non-aromatic" analog of the aromatic coordination compound is not available for direct comparison. This

approach harnesses the previously reported effect, using theoretical methods, where a Lewis base coordinated to the metal in a metalloaromatic compound breaks the aromaticity (Chart 1). Here, using a series of Lewis bases with varied donicity predicted chemical shifts for the unaccessible, non-aromatic analogs of SP Group 13 compounds are extrapolated. The chemical shift from the hypothetical, non-aromatic analogs to the aromatic SP compounds ranges between 0.22 – 0.41 ppm downfield.

Chart 1. Line drawing of the almost uniform bond lengths in  $(PDI^{2-})MX$  (left) and the alternating bond lengths in  $(PDI^{2-})AIX(Y)$  (right). M = AI, Ga; X = H, CI, I.

Previously reported computational work has discussed a role for aromaticity, along with ligand strain, in providing an energetic stabilization for SP  $\bf 1$  and  $\bf 4$ ,  $^{18b}$  following our report on the synthetic chemistry that yielded SP  $\bf 1$  and  $\bf 2$ .  $^{5b}$  In that work calculated NICS values for pyridine were compared with NICS values of the pyridyl ring in  $\bf 1$ , with NICS values for a hypothetical alumino-imidazolate, and with the metallo-imidazolate ring in  $\bf 1$  and  $\bf 4$  (Chart 2). The pyridyl ring in  $\bf 1$  showed decreased aromaticity relative to pyridine, and the metallo-imidazolate rings in  $\bf 1$  and  $\bf 4$  had NICS( $\bf 1$ )<sub>zz</sub> values of -7.3 and -8.2 ppm, respectively. No discussion of possible aromaticity in the outer 10-membered ring of the metal-ligand complexes was provided. These results suggested that a SP Ga complex  $\bf 4$  should have slightly greater aromatic character than  $\bf 1$ .

Chart 2. Previously computed NICS(1)<sub>zz</sub> values for pyridine, alumino-imidazolate, pyridyl in 1 (ring A), and metallo-imidazolate in 1 and 4 (ring B).  $^{18b}$ 

#### RESULTS AND DISCUSSION

**Syntheses of Compounds.** Synthesis of SP Al(III) complexes, (PDI<sup>2</sup>-)AlH (1) and (PDI<sup>2</sup>-)AlCl (2), has previously been reported via a salt metathesis route where AlCl<sub>2</sub>H, <sup>19</sup> or AlCl<sub>3</sub>, respectively, are added to a solution of Na<sub>2</sub>(PDI<sup>2</sup>-) generated in situ from Na metal and PDI in Et<sub>2</sub>O. <sup>13</sup> Error! Bookmark not defined. An extension of this preparative method was used to produce (PDI<sup>2</sup>-)AlI (3) using AlI<sub>3</sub>. The syntheses of Ga(III) complexes of reduced PDI ligands required care because both Ga(I) and Ga metal are readily accessible under the conditions which are required to reduce the PDI ligand by two electrons. Changes in the identity of the ethereal solvents, reactions times and work-up were required to isolate each of the new products and these nuances are detailed in

the Supporting Information. Synthesis of (PDI $^2$ -)GaH (4) using GaCl $_2$ H,  $^{20}$  which is generated in situ from GaCl $_3$  and 0.33 equivalents of LiAlH $_4$ , was achieved similarly to the syntheses of 1 - 3 (Scheme 1). In our initial efforts to obtain (PDI $^2$ -)GaCl (5), we routinely produced Ga mirrors from reactions containing PDI, Na, and GaCl $_3$  regardless of the order of addition of reagents or solvent employed. A reliable, but low yielding synthesis of 5 was achieved when "Na $_2$ (PDI $^2$ -)" in toluene was added dropwise over one hour to an Et $_2$ O solution of GaCl $_3$  at -78 °C.

## Scheme 1. Synthesis of 1 - 5. Ph = phenyl, Ar = diisopropylphenyl.

Complexes 3 - 5 were characterized using elemental analysis, and proton NMR spectra confirmed that each compound is diamagnetic with the expected proton resonances arising from the diisopropylphenyl and phenyl substituents. One pyridyl proton resonance appears as a triplet at 5.98. 6.16 and 6.08 ppm for 3 - 5, respectively, similar to those observed at 6.07 and 5.93 ppm for 1 and 2, respectively (Figure S1). The predicted doublet for the remaining two chemically equivalent pyridyl protons is obscured by the Ph and Ar substituents. UV-Vis-NIR spectra of 1 - 5 were collected in benzene and each demonstrate intense absorption bands with energy and extinction coefficients consistent with assignment as ligand-metal charge transfer bands (LMCT). Observation of these distinctive bands provides some support for assignment of an aromatic electronic structure for each of 1 - 5 (Figures S2, S3).6

Uncharged PDI ligand complexes of Al(III) and Ga(III) were also prepared to enable a comparison of bond lengths and angles with the anionic PDI ligands in  ${\bf 1}$  -  ${\bf 5}$ . Reaction of two equivalents of AlCl $_3$  or GaCl $_3$  with 1 equivalent of PDI in Et $_2$ O yielded [(PDI)AlCl $_2$ ][AlCl $_4$ ] (6) and [(PDI)GaCl $_2$ ][GaCl $_4$ ] (7), respectively, which were characterized using  $^1$ H,  $^{13}$ C NMR and UV-Vis-NIR spectroscopy (Figures S1 – S3), combustion analyses, and single crystal X-ray crystallography. The  $^1$ H NMR spectra of 6 and 7 display a single multiplet and pair of doublets from the diisopropyl substituents and the expected signals for the pyridyl, aryl, and phenyl substituents (Figure S1), as in reports of similar compounds.  $^{21}$  There is no observed LMCT band in the UV-vis/NIR spectra (Figures S2, S3).

**Solid-state structures.** Single crystals of  $\bf 3$  -  $\bf 7$  were used to characterize solid-state structures, and  $\bf 1$  and  $\bf 2$  were previously characterized. (Tables S1 - S4, Figures 1, S4, S5). For  $\bf 1$  -  $\bf 5$  single-crystal X-ray diffraction studies revealed approximately SP coordination about each metal center, and the four coordinate geometric indices  $(\tau_4)^{22}$  for  $\bf 1$  -  $\bf 5$  are 0.13, 0.22, 0.21, 0.18 and 0.22, where 0 would be an ideal SP molecule and 1 is tetrahedral (Table 1). In each of  $\bf 2$ ,  $\bf 3$  and  $\bf 5$  the halide ligand sits above the square plane and  $N_{py}$ -M-X

angles range from 167.01(4) to 168.78(19)°. The chloro and iodo ligands are  $\pi\text{-donating}$  and we speculate that the deviation from 180° enables the halide  $\pi\text{-donor}$  orbitals to interact with the  $\pi^*$  molecular orbital of the Al center. The hydrido ligand in 1 and 4 is a  $\sigma\text{-donor}$  only and no energetic stabilization would be achieved by distortion above the plane SP: 1 and 4 have Npy-M-H angles 180(1) and 177(11)°, respectively, which give the correspondingly lower values of  $\tau_4$  in those compounds (Table 1).

Table 1. Geometric and electronic parameters for 1 - 5. C.R. indicates chemical reaction.

	τ4	N <sub>py</sub> -M-X	N <sub>am</sub> -M-N <sub>am</sub>	Δδ (H <sub>Py</sub> )	Δδ ( <sup>31</sup> P)
1	0.13	180(1)	161.93(4)		23.2
2	0.22	167.01(4)	161.33(5)	0.22	25.0
3	0.21	168.8(2)	161.5(2)	0.41	C.R.
4	0.18	177(11)	158.35(11)		24.9
5	0.22	168.4(2)	161.11(15)		23.4

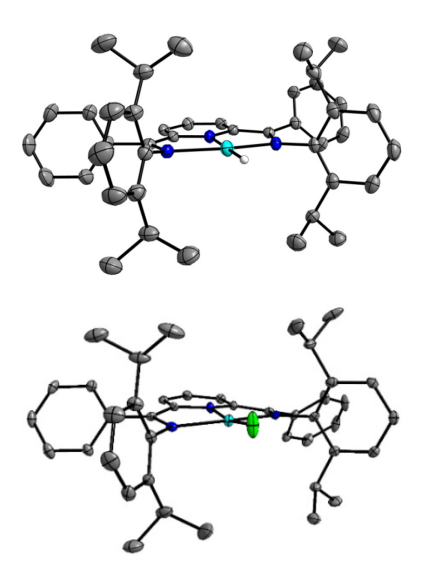


**Figure 1.** Solid-state structures of (PDI<sup>2</sup>-)GaH in **4** (top) and of (PDI<sup>2</sup>-)GaCl in **5** (bottom). Light blue, blue, green, and gray ellipsoids and white circle represent Ga, N, Cl, C, and H atoms, respectively. Thermal ellipsoids at 50% probability, H atoms except hydrido ligand omitted.

In the pyridyl rings of 1 - 5, the range over which the C-C bond lengths vary is just 0.0172, 0.013, 0.030, 0.018, and 0.019 Å for **1** – **5**, respectively. As a comparison it is known that alternating single and double bond character is observed in five-coordinate complexes of Al with the PDI<sup>2-</sup> ligand (Chart 1), 18 although the corresponding Ga complexes have not been isolated. Five-coordinate Al complexes with PDI2- ligands also have one Cim-Nim double and one Cim-Nim single bond whereas 1 - 5 have near equivalent Cim-Nim bond lengths on each side of the molecule: as an example, in 3 and 5 those bond lengths are 1.375(7)/1.374(7) and 1.368(6)/1.374(6) Å, respectively ( $C_{im}$  and  $N_{im}$  are the C and N atoms of the ligand imine functional group). In 6 and 7 with neutral PDI ligands those Cim-Nim bond lengths are shorter than in 1 - 5 which reflect the lower occupancy of the  $C_{im}$ - $N_{im}$   $\pi^*$  orbital (Figure S6). All of these observations are consistent with aromaticity providing an energetic preference for the unusual SP geometry.

An experimental probe of aromaticity. It is well-established for organic molecules that the ring current generated by an aromatic electronic structure causes a downfield chemical shift in the proton NMR spectrum for the protons bonded to carbon atoms of the aromatic ring. To observe evidence of a ring-current effect in a metal-containing aromatic compound can be difficult because the magnitude of the deshielding effect is usually small, and because the nonaromatic analog of the molecule is synthetically inaccessible. For these reasons, there is a heavy reliance on density functional theory (DFT), and canonical molecular orbital (CMO) nucleus-independent chemical shift (NICS),<sup>23</sup> harmonic oscillator model of aromaticity (HOMA),<sup>24</sup> and anisotropy of the current-induced density (ACID) computations, <sup>25</sup> when making assignments of aromaticity for metalcontaining ring systems.

To explore a simple experimental method for determination of aromaticity we probed the NMR chemical shifts of one pyridyl proton (denoted as H<sub>py</sub> in Chart 1) in **1 – 5** over a series of five-coordinate Al and Ga complexes where a fifth ligand was added (denoted as Y in Chart 1) and its Lewis basicity varied over a range of donicity values  $(-\Delta H^{\circ}_{BF3})$ .<sup>26</sup> We reasoned that a plot of  $\delta(H_{Pv})$  vs.  $-\Delta H^{\circ}_{BF3}$  could be extrapolated to obtain an estimated chemical shift for a SP complex coordinated to a theoretical Lewis base of donicity 0 kJ/mol: this value of  $\delta(H_{Py})$  is equivalent to the theoretical chemical shift of the non-aromatic SP analogs of 1 - 5. In a typical experiment, one of 1 - 5 was mixed with 1 equivalent of Lewis base in 0.4 mL of C<sub>6</sub>D<sub>6</sub> and the solution was stirred for 30 min before the proton NMR spectrum was collected. If an equilibrium between 1 - 5 and a Lewis base formed it would appear as a single average resonance and so we also collected NIR spectra of each solution in order to establish whether complete conversion to the five-coordinate adduct had occurred (Table S5, S6, Figures S3, S7-S14). In just a few cases, up to 50 equivalents of Lewis base was added before quantitative conversion to the solvated adduct was observed (Tables 2, S7 – S9, Figure S15).

Table 2. PDI pyridyl proton NMR chemical shifts,  $\delta(H_{py})$ , for 3 and 3-base as a function of base donicity,  $-\Delta H^{\circ}_{BF3}$ .

3·base	-∆H° <sub>BF3</sub> (kJ/mol)	∂(H <sub>py</sub> ) (ppm)	<sup>1</sup> H NMR spectrum of H <sub>py</sub>
N	134.17	5.36	
N_	128.08	5.34	M
	90.40	5.48	
N	60.95	5.46	
—≡N	60.39	5.46	
Ph≋N	55.44	5.50	
3 only		5.98	
			6.0 5.8 5.6 5.4 ppm

Chemical reaction of 1 and 4 with most of the Lewis bases employed precluded an estimation of  $\Delta \delta$ , and those reactions of Group 13 hydrido complexes, 1 and 4, with various nitriles and pyridines are consistent with prior reports.<sup>27,28</sup> Complexes 2 and 3 readily formed five-coordinate adducts with Lewis bases having  $-\Delta H^{\circ}_{BF3}$  spanning 60 - 130 kJ/mol (Figures S13, S14). The plot of  $\delta(H_{Py})$  vs.  $-\Delta H^{\circ}_{BF3}$  for each compound was fit with a straight line that passes through  $-\Delta H^{\circ}_{BF3} = 0$  at 5.71 and 5.57 ppm for 2 and 3, respectively (Figure 2). SP 2 and 3 have  $\delta(H_{Pv})$  of 5.93 and 5.98 ppm, respectively and therefore, the downfield chemical shift induced by the ring current in **2** and **3** is estimated as  $\Delta \delta = 0.22$  and 0.41 ppm, respectively. This small shift is in agreement with small NICS values for the pyridyl ring in 1 that were calculated in theoretical studies of SP Al complexes. 18b If there is a minor error introduced by sub-quantitative conversion to the solvated adduct of 2 or 3 in any data point it would result in a very small under-estimation of the ring current effect. Potential effects on NMR chemical shift caused by small changes in metal coordination sphere are likely accounted for in the correlation line but should not be completely discounted or forgotten.

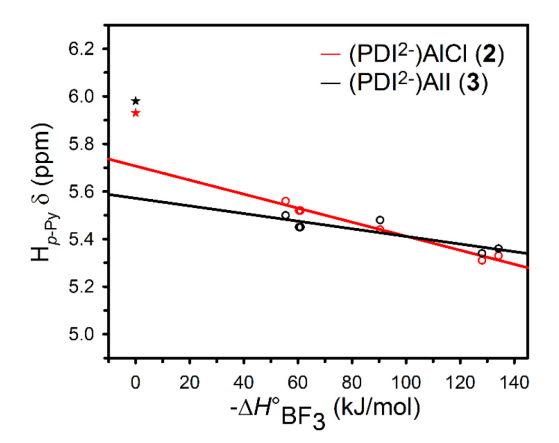


**Figure 2.** Plot of  $\delta(H_{Py})$  vs.  $-\Delta H^{\circ}_{BF3}$  for **2** (red), **3** (black), and **5** (blue). Each data point was obtained from a solution of **2**, **3**, or **5** with a Lewis base (Tables S6-S8, Figures S12, S13). Stars (\*) represent experimentally determined  $\delta(H_{Py})$  for SP **2**, red R<sup>2</sup> = 0.98; and **3**, black R<sup>2</sup> = 0.81.

The combined proton NMR and NIR spectroscopic experiments used to probe the dependence of  $\delta(H_{Py})$  on  $-\Delta H^{\circ}_{BF3}$ for 5 showed that it interacts with only the most donating bases that have  $-\Delta H^{\circ}_{BF3} > 120 \text{ kJ/mol}$  (Figure S14). Further, 50 equivalents of py were added to a solution of 5 in benzene before a near-quantitative conversion to 5.py was observed (Figure S15). Based on these data we were unable to estimate the ring current effect on chemical shift,  $\Delta\delta(H_{Pv})$ , for 5. A comparison of the HPy NMR chemical shifts for 2, 2.py, 5 and 5.py shows that the downfield chemical shift observed for SP 2 and 5 relative to 2·py and 5·py is 0.62 and 0.70 ppm, respectively (Figure 2, Tables S6-S9): this observation is consistent with, although not proof of, enhanced aromaticity in 5 relative to 2. Prior theoretical work on aluminepin and gallepin has shown that the Ga analog has a greater aromatic character that corresponds to a lower driving force for gallepin to bind solvent molecules, 14b and prior theoretical work on 1 and 4 predicted greater aromatic character for 4.17b These observations suggest that

the analysis method we have presented for estimating aromatic chemical shifts, may not be useful in cases where a large energetic stabilization is derived from the aromaticity.

We also reasoned that the Lewis acidity of the Al and Ga centers in 1 - 5 should be lower than expected for non-aromatic Al(III) and Ga(III) complexes. To benchmark the Lewis acidity of 1 - 5 against other known Lewis acidic compounds we monitored the <sup>31</sup>P NMR chemical shift of Et<sub>3</sub>PO in the presence of 1 - 5, as others have done.<sup>29</sup> All of the <sup>31</sup>P NMR resonances were observed between 68.8 and 70.7 ppm, except for 3 for which the data were discarded since a reaction was observed (Table 1, Figure S16). This data shows that the Lewis acidity does not change much across **1** – **5**, and that the Lewis acidity decreases in the order  $2 \ge$  $4 > 1 \ge 5$  which does not reflect the expectation that Al(III) complexes are more Lewis acidic than Ga(III) complexes. In previous reports, four- and three-coordinate Al complex adducts with Et<sub>3</sub>PO have been characterized with <sup>31</sup>P NMR chemical shifts observed at 83.4 and 81.5 ppm, respectively.30,31 The observations made herein are consistent with significant ligand-metal charge transfer character and an aromatic electronic structure which lowers the Lewis acidity of 1 - 5 relative to other known three- and four-coordinate Al compounds.

The aromatic electronic structure model for **1** - **5** can also be used to rationalize the reactivity properties of Group 13 complexes of PDI: these reactivity properties alone are not confirmation of aromaticity. For example, addition of acids (p $K_a$  values 5 – 24) to **1** protonates a ligand N-donor atom and does not react with the hydrido ligand to produce H<sub>2</sub> (Scheme 2).10 This reactivity may be attributable to the aromatic character of 1 since increased nucleophilicity of the ligand chelate ring would promote the ligand protonation, and aromatic character on the Al center should lower the hydricity of the hydrido ligand. Reports of other Group 13 hydrido complexes confirm that Al- and Ga-hydrides generally display facile reactions with weak acids to liberate H<sub>2</sub> even when those complexes contain anionic N-donor ligands.<sup>32</sup> Protonation of **2** also has been shown to occur at the ligand amido donor, although in that case there is no competing Al-hydrido which "should" be protonated.5b

### Scheme 2. Summary of previously reported reactions of 1 with aniline. 10 Ph = phenyl, Ar = diisopropylphenyl.

Analogous experiments were performed with 4 and 5: one equivalent of aniline was added to a benzene solution of each compound, and the solution turned bright blue from a dark brown color. The observed color change exactly parallels the changes observed when 1 and 2 were protonated at the ligand and suggests that the same reaction has

occurred here: we were unable to crystallize these compounds or to isolate pure samples. Characterization using proton NMR spectroscopy suggested that an equilibrium protonation of the amido *N*-atom precludes isolation of the products (Figure S17-S19).

The reactivity and spectroscopic properties of *d*-block PDI complexes are more varied and generally do not support their assignment as aromatic. Using Fe complexes of PDI<sup>2-</sup> as examples, there are five known SP compounds: Li[(PDI<sup>2</sup>-)FeMel.<sup>33</sup> (PDI<sup>2-</sup>)Fe(DMAP),<sup>34</sup> (PDI<sup>2</sup>-)Fe( $\eta^4$ -1,3-butadiene),<sup>36</sup> )FeN<sub>2</sub>CHSi(CH<sub>3</sub>)<sub>3</sub>,<sup>35</sup> and (PDI<sup>2</sup>-)Fe( $\eta^3$ -hex-1-en-6-yl). <sup>37</sup> In general, antiferromagnetic coupling between ligand radicals and unpaired electrons on the Fe center is observed, and this must be a lower energy structure which is not available to Group 13 complexes. We conclude that the reactivity and electronic properties of Group 13 PDI complexes and those of *d*-block elements is distinct as a result of the differences in their electronic structures.

In conclusion, examples of SP Ga(III) complexes are reported and their aromatic character is examined. The aromatic character is manifested in downfield chemical shifts of the ligand proton NMR resonances. We further demonstrated that proton NMR experiments performed with 2, and 3, and a series of Lewis bases with varied donicity can be employed to probe the chemical shift caused by deshielding of protons by ring-current: this is a potentially general and very simple experimental probe of metalloaromaticity. In cases where chemical reactions occur with the donor Lewis base, or in cases where aromatic stabilization is large so that donors do not bind the metal then this method may not be useful. Low energy LMCT bands observed using NIR

spectroscopy further support the model where ligand electron density is shared with the Al and Ga centers. The aromatic electronic structure model has aided in rationalization of the observed geometric, electronic, and reactivity properties of  ${\bf 1}-{\bf 5}$ , and will aid with future efforts to develop and predict the chemistry and reactivity of Group 13 PDI complexes.

#### **ASSOCIATED CONTENT**

#### **Supporting Information.**

Experimental methods, NMR and UV-Vis-NIR spectra, fits to data, crystallographic data (PDF)

Crystallographic data (CIF)

This material is available free of charge via the Internet at http://pubs.acs.org.

#### **AUTHOR INFORMATION**

#### **Corresponding Author**

laberben@ucdavis.edu\*

#### **Author Contributions**

All authors have given approval to the final version of the manuscript.

#### **ACKNOWLEDGMENT**

This manuscript is based on work supported by the National Science Foundation with grant CHE-1763821. We thank Prof. H. B. Gray for an insightful discussion and Prof. S. M. Kauzlarich for use of a UV-Vis-NIR spectrometer.

#### **REFERENCES**

 $^1$  For example: a) Dohmeier, C.; Robl, C.; Tacke, M.; Schnöckel, H. The Tetrameric Aluminum(I) Compound [{Al( $\eta^5\text{-}C_5\text{Me}_5)\}_4$ ]. *Angew. Chem. Int. Ed.* **1991**, *30*, 564-565. b) Cui, C.; Roesky, H. W.; Schmidt, H.-G.; Noltemeyer, M.; Hao, H.; Cimpoesu, F. Synthesis and Structure of a Monomeric Aluminum(I) Compound [{HC(CMeNAr)}\_2}Al] (Ar=2,6-I Pr\$\_2C\_6H\_3): A Stable Aluminum Analogue of a Carbene. *Angew. Chem. Int. Ed.* **2000**, *39*, 4274-4276.

Tris(triphenylphosphine)aluminum Ambiphilic Precatalyst for the Reduction of Carbon Dioxide with Catecholborane. *Organometallics.* **2013**, *32*, 6804-6811.

- <sup>4</sup> Arnold, A.; Sherbow, T. J.; Sayler, R. I.; Britt, R. D.; Thompson, E. J.; Munoz, M. T.; Fettinger, J. C.; Berben, L. A. Organic Electron Delocalization Modulated by Ligand Charge State in  $[L_2M]^n$  Complexes of Group 13 Ions. *J. Am. Chem. Soc.* **2019**, *141*, 15792–15803.
- <sup>5</sup> a) Myers, T. W.; Berben, L. A. Aluminum-Ligand Cooperative N-H Bond Activation and an Example of Dehydrogenative Coupling. *J. Am. Chem. Soc.* **2013**, *135*, 9988-9990. b) Thompson, E. J.; Meyers, T. W.; Berben, L. A. Synthesis of Square-Planar Aluminum(III) Complexes. *Angew. Chem. Intl. Ed.* **2014**, *53*, 14132-14134. c) Thompson, E. J.; Berben, L. A. Electrocatalytic Hydrogen Production by an Aluminum(III) Complex: Ligand-Based Proton and Electron Transfer. *Angew. Chem. Intl. Ed.* **2015**, *54*, 11642-11646.
- <sup>6</sup> Gomes, J. A. N. F.; Mallion, R. B. Aromaticity and Ring Currents. *Chem. Rev.* **2001**, *101*, 1349-1384.
- <sup>7</sup> Masui, H. Metalloaromaticity. *Coord. Chem. Rev.* **2001**, *219-221*, 957-992.
- $^8$  a) Baudler, M. Polyphosphorous Compounds–New Results and Perspectives. *Angew. Chem. Int. Ed.* **1987**, *26*, 419-441. b) Scherer, O. J.; Brück, T. [( $\eta^{-5}$ - $P_5$ )Fe( $\eta^{5}$ - $C_5$ Me<sub>5</sub>)], a Pentaphosphaferrocence Derivative. *Angew. Chem. Int. Ed.* **1987**, *26*, 59-59.
- $^9$  Velian, A.; Cummins, C. C. Synthesis and characterization of  $P_2N_3$ : An aromatic ion composed of phosphorus and nitrogen. *Science.* **2015**, *348*, 1001-1004.

<sup>&</sup>lt;sup>2</sup> a) Hicks, J.; Vasko, P.; Goicoechea, J. M.; Aldridge, S., The Aluminyl Anion: A New Generation of Aluminium Nucleophile. *Angew. Chem. Int. Ed.* DOI:10.1002/anie.202007530. b) Hicks, J.; Vasko, P.; Goicoechea, J. M.; Aldridge, S., Synthesis, structure and reaction chemistry of a nucleophilic aluminyl anion. *Nature* **2018**, *557*, 92-95. c) Schwamm, R. J.; Anker, M. D.; Lein, M.; Coles, M. P., Reduction vs. Addition: The Reaction of an Aluminyl Anion with 1,3,5,7-Cyclooctatetraene. *Angew. Chem. Int. Ed.* **2019**, *58*, 1489-1493. d) Kurumada, S.; Takamori, S.; Yamashita, M., An alkyl-substituted aluminium anion with strong basicity and nucleophilicity. *Nat. Chem.* **2020**, *12*, 36-39. e) Koshino, K.; Kinjo, R., Construction of σ-Aromatic AlB<sub>2</sub> Ring via Borane Coupling with a Dicoordinate Cyclic (Alkyl)(Amino)Aluminyl Anion. *J. Am. Chem. Soc.* **2020**, *142*, 9057-

<sup>&</sup>lt;sup>3</sup> For example: a) Stephan, D. W. The broadening reach of frustrated Lewis pair chemistry. *Science* **2016**, *354*, 1248-1257. b) Appelt, C.; Slootweg, J. C.; Lammertsma, K.; Uhl, W. Reaction of a P/Al-Based Frustrated Lewis Pair with Ammonia, Borane, and Amine–Boranes: Adduct Formation and Catalytic Dehydrogenation. *Angew. Chem. Int. Ed.* **2013**, *52*, 4256-. c) Courtemanche, M.-A.; Larouche, J.; Légaré, M.-A.; Bi, W.; Maron, L.; Fontaine, F.-G. A

- <sup>10</sup> Myers, T. W.; Berben, L. A. Aluminum-Ligand Cooperative N-H Bond Activation and an Example of Dehydrogenative Coupling. *J. Am. Chem. Soc.* **2013**. *135*. 9988-9990.
- <sup>11</sup> Zhu, C.; Li, S.; Luo, M; Zhou, X.; Niu, Y.; Lin, M.; Zhu, J.; Cao, Z.; Lu, X.; Wen, T.; Xie, Z.; Schleyer, P. v. R.; Xia, H. Stabilization of antiaromatic and strained five-membered rings with a transition metal. *Nat Chem.* **2013**, *5*, 698 -703.
- <sup>12</sup> Gray, H. B.; Ballhausen, C. J. A Molecular Orbital Theory for Square Planar Metal Complexes. *J. Am. Chem. Soc.* **1963**, *85*, 260-265.
- <sup>13</sup> Billig, E.; Williams, R.; Bernal, I.; Waters, J. H.; Gray, H. B. The Electronic Structures of Square-Planar Metal Complexes of Maleonitriledithiolate with Copper(II), Nickel(II), Palladium(II), and Platinum(II). *Inorg. Chem.* **1964**, *3*, 663-666.
- <sup>14</sup> Tovar, D.; Messersmith, R. E.; Borepin Rings as "Sigma-Free" Reporters of Aromaticity within Polycyclic Aromatic Scaffolds. *J. Phys. Chem. A.* **2019**, *123*, 881-888. b) Yoshida, K.; Furuyama, T.; Wang, C.; Muranaka, A.; Hashizume, D.; Yasuike, S.; Uchiyama, M. Aluminepin: Aluminum Analogues of Borepin and Gallepin. *J. Org. Chem.* **2012**, *77*, 729-732. c) Quillian, B.; Wang, Y.; Wei, P.; Wannere, C. S.; Schleyer, P. v. R.; Robinson, G. H. Gallepins. Neutral Gallium Analogues of the Tropylium Ion: Synthesis, Structure, and Aromaticity. *J. Am. Chem. Soc.* **2007**, *129*, 13380-13381.
- <sup>15</sup> Nakamura, T.; Suzuku, K.; Yamashita, M. An Anionic Aluminabenzene bearing Aromatic and Ambiphilic Contributions. *J. Am. Chem. Soc.* **2014**, *136*, 9276-9279.
- <sup>16</sup> Cao, X. Y.; Zhao, Q.; Lin, Z.; Xia, H. The Chemistry of Aromatic Osmacycles. *Acc. Chem. Res.* **2014**, *47*, 341–354.
- <sup>17</sup> Saito, M. Transition-Metal Complexes Featuring Dianionic Heavy Group 14 Element Aromatic Ligands. *Acc. Chem. Rev.* **2018**, *51*, 160 169.
- <sup>18</sup> a) Chen, Z.; Wang, W.; Zhu, C.; Wang, L.; Fang, X.; Qiu, Y. Probing chemical bonding and optoelectronic properties of Square-Planar Aluminum, Gallium, and Nickel Complexes. *Comput. Theor. Chem.* **2016**, *1090*, 129-133. b) Li, W.; Lyu, Y.; Zhang, H.; Zhu, M.; Tang. H. A theoretical study on the unusual square-planar structure of bis(imino)pyridine-ligated Group 13 complexes. *Dalton Trans.* **2017**, *46*, 106-115.
- <sup>19</sup> Schmidt, D. L.; Flagg, E. E. Bis(tetrahydrofuran)-haloalanes *Inorg. Chem.* **1967**, *6*, 1262-1265.
- <sup>20</sup> Nogai, S.; Schmidbaur, H. Dichlorogallane (HGaCl<sub>2</sub>)<sub>2</sub>: Its Molecular Structure and Synthetic Potential. *Inorg. Chem.* **2002**, *41*, 4770-4774.
- <sup>21</sup> Jurca, T.; Dawson, K.; Mallov, I.; Burchell, T.; Yap, G. P. A.; Richeson, D. S. Disproportionation and radical formation in the coordination of "Gal" with bis(imino)pyridines. *Dalton Trans.*, **2010**, *39*, 1266-1272.
- $^{22}$  Yang, L.; Powell, D. R.; Houser, R. P. Structural variation in copper(I) complexes with pyridylmethylamide ligands: structural analysis with a new four-coordinate geometry index,  $\tau_4$ . *Dalton Trans.* **2007**, 955-964.
- $^{23}a)$  Schleyer, P. v. R.; Maerker, C.; Dransfeld, A.; Jiao, H.; Hommes, N. J. R. v. E. Nucleus-Independent Chemical Shifts: A Simple and Efficient Aromaticity Probe. *J. Am. Chem. Soc.* **1996**. *118*, 6317–6318. b) Chen, Z.; Wannere, C. S.; Corminboeuf, C.; Puchta, R.; Schleyer, P. v. R. Nucleus-Independent Chemical Shifts (NICS) as an Aromaticity Criterion. *Chem. Rev.* **2005**. *105*, 3842–3888. c) Fallah-Bagher-Shaidaei, H.; Wannere, C. S.; Corminboeuf, C.; Puchta, R.; Schleyer, P. v. R. Which NICS Aromaticity Index for Planar  $\pi$  Rings is Best? *Org. Lett.* **2006**, *8*, 863–866.

- <sup>24</sup> Kruszewski, J.; Krygowski, T. M. Definition of Aromaticity Basing on the Harmonic Oscillator Model. *Tetrahedron Lett.* **1972**, *13*, *36*, 3839-3842.
- <sup>25</sup> Herges, R.; Geuenich, D. Delocalization of Electrons in Molecules. *J. Phys. Chem.* **2001**, *105*, *13*, 3214-3220.
- <sup>26</sup> a) Maria, P. C.; Gal, J.-F. A Lewis basicity scale for non-protogenic solvents: enthalpies of complex formation with boron trifluoride in dichloromethane. *J. Phys. Chem.* **1985**, *89*, 1296-1304. b) Laurence, C.; Graton, J.; Gal, J.-F. An Overview of Lewis Basicity and Affinity Scales. *J. Chem. Educ.* **2011**, *88*, 1651-1657.
- <sup>27</sup> Lansbury, P. T.; Peterson, J. O.; Lithium Tetrakis-(N-dihydropyridyl)-aluminate: Structure and Reducing Properties. *J. Am. Chem. Soc.*, **1963**, *85*, 2236–2237.
- <sup>28</sup> Amundsen, L. H.; Nelson, L. S.; Reduction of Nitriles to Primary Amines with Lithium Aluminum Hydride. *J. Am. Chem. Soc.* **1951**, 73, 1, 242–244.
- <sup>29</sup> Beckett, M. A.; Strickland, G. C.; Holland, J. R.; Varma, K. S. A convenient n.m.r. method for the measurement of Lewis acidity at boron centres: correlation of reaction rates with Lewis acid initiated epoxide polymerizations with Lewis acidity. *Polymer.* **1996**, *37*, 4629–4631.
- <sup>30</sup> Wang, C.; Lin, Y.; Tseng, H.; Lee, G.; Peng, S.; Chiu, C. N-Heterocyclic Carbene Complexes of Cp\*-Aluminum Triflate. *Eur. J. Inorg. Chem.* **2018**, *20-21*, 2232-2236.
- <sup>31</sup> Stennett, T. E.; Pahl, J.; Zijlstra, H. S.; Seidel, F. W.; Harder, S. A. Frustrated Lewis Pair Based on a Cationic Aluminum Complex and Triphenylphosphine. *Organometallics*. **2016**, *35*, 207-217.
- <sup>32</sup> a) Wehmschulte, R. J.; Power, P. P. Reactions of (H<sub>2</sub>AlMes\*)<sub>2</sub> (Mes\* = 2,4,6-(t-Bu)<sub>3</sub>C<sub>6</sub>H<sub>2</sub>) with H<sub>2</sub>Ear (E = N, P, or As; Ar = aryl): Characterization of the Ring Compounds (Mes\*AlNHPh)<sub>2</sub> and (Mes\*AlEPh)<sub>3</sub> (E = P or As). *J. Am. Chem. Soc.* **1996**. *118*. 791–797. b) Wehmschulte, R. J.; Power, P. P. Reaction of the Primary Alane (2,4,6-t-Bu<sub>3</sub>H<sub>2</sub>C<sub>6</sub>AlH<sub>2</sub>)<sub>2</sub> with Nitriles, Isonitriles, and Primary Amines. *Inorg. Chem.* **1998**, 37, 26, 6906–6911. c) Mills, D. P.; Rose, R. P.; Jones, C. Oxidative addition of an imidazolium cation to an anionic gallium(I) *N*-heterocyclic carbene analogue: Synthesis and characterisation of novel gallium hydride complexes. *J. Organomet. Chem.* **2006**, 691. 3060–3064.
- <sup>33</sup> Scott, J.; Gambarotta, S.; Korobkov, I.; Budzelaar, P. H. M. Reduction of (Diiminopyridine)iron: Evidence for a Noncationic Polymerization Pathway? *Organometallics.* **2005**, *24*, *26*, 6298-6300.
- <sup>34</sup> Bart, S. C.; Chlopek, K.; Bill, E.; Bouwkamp, M. W.; Lobkovsky, E.; Neese, F.; Wieghardt, K.; Chirik, P. J. Electronic Structure of Bis(imino)pyridine Iron Dichloride, Monochloride, and Neutral Ligand Complexes: A Combined Structural, Spectroscopic, and Computational Study. *J. Am. Chem. Soc.* **2006**, *128*, *42*, 13901-13912.
  - 35 Tondreau, A. M.; Milsmann, C.; Patrick, A. D.; Hoyt, H. M.;
- Lobkovsky, E.; Wieghardt, K.; Chirik, P. J. Synthesis and Electronic Structure of Cationic, Neutral, and Anionic Bis(imino)pyridine Iron Alkyl Complexes: Evaluation of Redox Activity in Single-Component Ethylene Polymerization Catalysts. *J. Am. Chem. Soc.* **2010**, *132*, *42*, 15046-15059.
- <sup>36</sup> Bouwkamp, M. W.; Bowman, A. C.; Lobkovsky, E.; Chirik, P. J. Iron-Catalyzed  $[2\pi + 2\pi]$  Cycloaddition of  $\alpha,\omega$ -Dienes: The Importance of Redox-Active Supporting Ligands. *J. Am. Chem. Soc.* **2006**, *128*, *41*, 13340-13341.
- $^{37}$  Russell, S. K.; Lobkovsky, E.; Chirik, P. J. Iron-Catalyzed Intermolecular [2 $\pi$  + 2 $\pi$ ] Cycloaddition. *J. Am. Chem. Soc.* **2011**, *133*, *23*, 8858-886.

### TOC Graphic

